Chinese Journal of Aeronautics, (2018), xxx(xx): xxx–xxx

Chinese Society of Aeronautics and Astronautics
& Beihang University

Chinese Journal of Aeronautics

cja@buaa.edu.cn
www.sciencedirect.com

FULL LENGTH ARTICLE

Scaling procedures of cabin noise generated by turbulent boundary layer excitation

Xiaojian ZHAO [a,*], Wei SONG [a], Jie ZHOU [b], Bangcheng AI [a]

[a] China Academy of Aerospace Aerodynamics, Beijing 100074, China
[b] University of Southampton, Southampton, England SO17IBJ, United Kingdom

Received 3 January 2017; revised 9 May 2017; accepted 28 June 2017

KEYWORDS

Cabin noise;
Scaling procedure;
Turbulent boundary layer;
Vibro-acoustic;
Wind tunnel

Abstract This paper presents a new method for measuring the cabin noise of a structure in a wind tunnel. A method for scaling the cabin sound was derived to obtain the cabin noise of a structure, and the derivation of the scaling procedure was based on a theoretical hypothesis regarding the cabin noise prediction for a scaled model in a wind tunnel. A frequency offset was generated because of the error introduced by model manufacture and installation, and a proposed modal test method was used to eliminate the frequency offset. Both a full-scale structure and scaled structure were measured in the wind tunnel tests. The cabin noise of the full-scale model was compared with the results obtained using the scaling procedure based on the scaled model. The comparisons of the measurement results indicate that the scaling procedures developed in this paper are effective for vibro-acoustic predictions in wind tunnels. Moreover, background noise tended to affect the results of the cabin sound for the wind tunnel test, and thus background noise should be prevented through specific design efforts.

1. Introduction

Interior noise alleviation is an issue of primary interest in the design of modern aircraft. The acoustic nuisance inside the cabin may adversely influence passenger comfort, particularly in helicopter and propeller-driven aircraft. The typical sources for generating cabin noise include the fuselage boundary layer and airborne and structure-borne noise, which may cause unacceptable ride discomfort and impact the fatigue life of the structure.

Investigations on the cabin noise induced by Turbulent Boundary Layers (TBLs) began early on. In Ref.[1], the contribution of TBLs to cabin noise was studied, and the problem was formulated as a sequence of two linear couplings, namely, the TBL fluctuations exciting the fuselage skin in lateral vibrations and the skin vibrations inducing sound inside the fuselage. Moreover, it was assumed that the boundary layer was locally homogeneous and the fuselage skin was flat, and only outgoing waves were considered. Airplane interior broadband noise under the cruise condition was considered to be dominated by the TBL. For the prediction of cabin noise, a mathematical model[2] was derived from the Statistical Energy

* Corresponding author.
E-mail address: zhaox0714@126.com (X. ZHAO).
Peer review under responsibility of Editorial Committee of CJA.

Production and hosting by Elsevier

https://doi.org/10.1016/j.cja.2017.12.015
1000-9361 © 2018 Chinese Society of Aeronautics and Astronautics. Production and hosting by Elsevier Ltd.

Please cite this article in press as: ZHAO X et al. Scaling procedures of cabin noise generated by turbulent boundary layer excitation, *Chin J Aeronaut* (2018), https://doi.org/10.1016/j.cja.2017.12.015

Analysis (SEA) technique to evaluate the interior TBL noise of a Boeing 737 airplane. A method for measuring the in-flight noise and vibration of an aircraft, developed by SAAB (Svenska Aeroplan AktieBolaget),[3] was shown to be a powerful tool for monitoring the quality of an aircraft. In Ref.[4], ground and flight measurements were conducted on a pusher-propeller configuration with different interior furnishings. The main objective of the measurements was to identify the sources of interior noise on a specific airplane and revise the computer program so that it could be used to predict the noise effects of interior treatment modifications. A new wavenumber-based approach for predicting sound transmission through an aircraft fuselage was introduced in Ref.[5]. The proposed method was accurate at mid-frequencies, for which the method involved nearly no approximation for a large doubly periodic panel. A new stochastic model of simulating the surface pressure fluctuations that induced cabin noise was developed in Ref.[6]. The method proved to be efficient when a random particle mesh method with recursive filters was used. Ref.[7] investigated the cabin noise generated by engine noise, and the proposed methodology considered the engine as a spatially extended source and assumed that the jet-mixing source was a line source distributed on the engine axis. With a focus on the cabin noise induced by TBL excitation, the interior noise environment in a Large Civil TiltrotoR (LCTR2) was assessed in Ref.[8]. The contributions of different aero-acoustic sources to the cabin noise of an aircraft, including the TBL, jet noise and the air conditioning system, were compared in Ref.[9]. Extensive measurements with microphones mounted at various longitudinal positions were used to assess the cabin noise. Ref.[10] presented the results of flight measurements, including the field of pressure fluctuation on the fuselage and cabin noise, and identified the main sources of noise.

The methods developed for assessing cabin noise typically only provide tools to support the noise control in the cabin of the aircraft. Ref.[11] reported the reduction of the engine rotor vibration-induced cabin noise of DC-9 due to several improvement designs. Ref.[12] investigated the control of low-frequency cabin noise and proposed a concept based on intrinsic tuning and damping of fuselage structural elements. Ref.[13] discussed the performance of various structural and cabin sidewall treatments applied to reduce cabin noise, and the measurement and analysis were conducted on a DC-9 test section. Passive vibration absorbers are often ineffective for the analysis of frequencies below 500 Hz because the wavelength is large compared to the thickness of a damping layer. Thus, an active control system for cabin noise consisting of actuators and sensors was used in Refs.[14–17].

The precision of the simulated TBL excitation typically limits the cabin noise assessment. A wind tunnel test is the most effective method for simulating TBL excitations over an aircraft with a scaled model. Thus, this paper proposes to assess the cabin noise of a craft induced by TBL excitation in a wind tunnel. Moreover, scaling laws are developed to relate the cabin noise of a scaled model with the full-scale model. The remainder of the paper is organized as follows. Section 2 describes the cabin noise scaling procedures, which are derived from the theoretical models of cylindrical shell vibrations induced by TBL excitations. Furthermore, to validate the derived scaling procedures, theoretical results are presented in Section 3. In Section 4, the measurements are introduced, and the experimental results are discussed in Section 5. The last section provides conclusions concerning the work in this paper.

2. A scaling procedure for cylindrical shell response

The scaling procedures used to predict the structural response of a typical aircraft when subjected to TBL excitations were derived based on a curved cylindrical shell (Fig. 1). In Fig. 1, a and b indicate the length and the width of the cylindrical shell, respectively, and R is the curvature. The scaling laws of the structure response induced by TBL excitation introduced in Section 2.1 were developed in Refs.[18,19] Because the interior sound distribution is also an important factor that must be considered in the structural design of an actual aircraft, the other scaling procedure was developed in Section 2.2 to relate the cabin noise distribution of scaled aircraft structures with that of full-scale aircraft structures. The scaling procedures developed can provide theoretical support for predicting cabin noise in a wind tunnel.

2.1. Scaling procedure of structure response

The differential equations governing the vibration of a curved cylindrical shell (as presented in Refs.[20,21]) are as follows:

$$D\nabla^4 w + \nabla_\kappa^2 w - \mu\omega^2 w = 2p^i - 2p^r \tag{1}$$

$$Eh\nabla_\kappa^2 w - \nabla^4 \zeta = 0 \tag{2}$$

where w is the transverse displacement of panel.

$\mu = \rho h$, which indicates the area density; h is the thickness of the curved cylindrical shell and ρ is the density of structure. $D = Eh^3/12(1-v^2)$, where v is Poisson's ratio of the shell, E is Young's modulus; $p^i = \exp[\mathrm{j}(\omega t - k_x x - k_y y - k_z z)]$, which indicates an incident wave acting on the shell, k_x, k_y, k_z are the wave number along x, y, z, respectively, p^r denotes the acoustic pressure radiated by the shell, ζ is Airy's stress function,ω is circular excitation frequency, t is the time, ∇_κ^2 indicates the second-order operator, ∇^4 indicates the forth-order operator, j is the imaginary unit.

If the scaling coefficient is denoted as σ, each side of the scaled curved cylindrical shell can be expressed as $\bar{a} = \sigma a$, $\bar{b} = \sigma b$, and $\bar{h} = \sigma h$. The parameters with ‾ correspond to the scaled model.

The relationship characterizing the velocity Power Spectral Density (PSD) response between the scaled model and the full-scale model is as follows:[18,19]

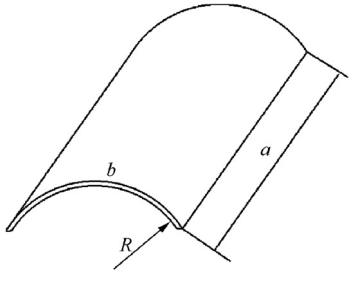

Fig. 1 Schematic of cylindrical shell.

$$S_v(\omega) = \frac{1}{\sigma}\cdot\frac{\bar{V}}{V}\left(\frac{q_\infty}{\bar{q}_\infty}\right)^2\left(\frac{\bar{L}}{L}\right)^2\bar{S}_v(\bar{\bar{\omega}}) \tag{3}$$

In addition, S_v is the velocity power spectral density of the structure, $\omega = \bar{\bar{\omega}}\bar{\sigma}$ which is circular frequency $\bar{\sigma} = \sigma\frac{G}{\bar{G}}$, and $L = G\rho = \rho\sqrt{\frac{E}{12\rho(1-\nu^2)}} = \sqrt{\frac{\rho E}{12(1-\nu^2)}}$, $\bar{\bar{\omega}}$ indicates the response frequency of the scaled model, V is free stream velocity, q_∞ is dynamic pressure of the flow.

2.2. Scaling procedure for internal sound

The internal sound assessment of the aircraft is based on a weak coupling approximation. The flow induces the structural vibration, and then the structural vibration determines the internal acoustic pressure; however, the counterforce of the sound pressure applied to the structure is ignored. The structural vibration of a curved cylindrical shell is more complex than the sound radiation of a flat plate. The internal sound pressure of an aircraft is typically determined based on two important sound source components: direct sound[21] and reverberation sound. The sound pressure at an arbitrary point in the cabin of an aircraft is expressed as

$$p(\omega, X) = p_z(\omega) + p_h(\omega) \tag{4}$$

where the direct sound $p_z(\omega) = \frac{\mathrm{i}\omega\rho_0}{2\pi}\int_S \frac{\dot{w}(X')\mathrm{e}^{-\mathrm{i}\bar{\bar{k}}r}}{r}\mathrm{d}X'$ and the reverberation sound $p_h(\omega) = \frac{\mathrm{i}\omega\rho_0}{2\pi}\int_S \frac{\dot{w}(X')\mathrm{e}^{-\mathrm{i}kr'}}{r'}\mathrm{d}X'$, X' indicates a point on the plate, S indicates the surface of the plate, k is the wave number, ρ_0 is the density of air in the cabin, r, r' indicate the trajectories of direct sound and reverberation sound, respectively, and $\dot{w}(X')$ is the vibration velocity of the aircraft panel.

When the aircraft is scaled, the direct sound can be expressed as

$$p_z(\omega) = \frac{\mathrm{i}\omega\rho_0}{2\pi}\int_S \frac{\dot{w}(X')\mathrm{e}^{-\mathrm{i}kr}}{r}\mathrm{d}X' = \frac{\mathrm{i}\bar{\bar{\omega}}\bar{\sigma}\rho_0}{2\pi}\int_S \frac{\dot{w}(X')\mathrm{e}^{-\mathrm{i}k\bar{r}\frac{\bar{\sigma}}{\sigma}}}{\bar{r}}\mathrm{d}\bar{X}' \tag{5}$$

According to the research presented in the paper discussed in Section 2.1,

$$\dot{w}(X') = K\dot{w}(\bar{X}')$$

where K indicates the velocity response relationship between the scaled model and the original structure, which is determined by the coefficients of the derived scaling procedures presented in Section 2.1. Eq. (3) presents the velocity PSD response relationship between the scaled model and the original structure. Therefore, the coefficient K could be obtained by combining Eq. (5) with Eq. (3).

Thus,

$$p_z(\omega) = \frac{\mathrm{i}\bar{\bar{\omega}}\bar{\sigma}\rho_0}{2\pi}\int_S \frac{K\dot{w}(\bar{X}')\mathrm{e}^{-\mathrm{i}\bar{\bar{k}}\bar{r}\frac{\bar{\sigma}}{\sigma}}}{\bar{r}}\mathrm{d}\bar{X}' = K\frac{\bar{\sigma}}{\sigma}\cdot\frac{\mathrm{i}\bar{\bar{\omega}}\rho_0}{2\pi}\int_{\bar{S}} \frac{\dot{w}(X')\mathrm{e}^{-\mathrm{i}\bar{\bar{k}}\bar{r}\frac{\bar{\sigma}}{\sigma}}}{\bar{r}}\mathrm{d}\bar{X}' \tag{6}$$

From Eq. (6), a scaling relationship between the direct sound of the scaled model and that of a full-dimensional model is obtained if either $\bar{\sigma}/\sigma = 1$ or $G = \bar{G}$ is satisfied. The scaling laws can be expressed as

$$p_z(\omega) = K\bar{p}_z(\omega)$$

In addition, the reverberation sound also satisfies a similar formula:

$$p_h(\omega) = K\bar{p}_h(\omega)$$

Thus, the following expression can be obtained:

$$p(\omega, X) = K\bar{p}_z(\omega) + K\bar{p}_h(\omega) \tag{7}$$

According to the research in Section 2.1, $K = \sqrt{\frac{1}{\sigma}\left(\frac{\bar{\rho}}{\rho}\right)^2\left(\frac{q}{\bar{q}}\right)^2\left(\frac{\bar{V}}{V}\right)}$ is obtained, q is the dynamical pressure of airflow.

3. Theoretical results

To validate the scaling laws developed regarding the cabin noise induced by TBL excitation, the Finite Element Method (FEM) solver in the VA-One software was used to compute the cabin noise of a typical aircraft layout (Fig. 2). The Corcos model used to simulate the TBL excitation can be expressed as[20]

$$S_p(\xi_x, \xi_y, \omega) = S_{pp}(\omega)\mathrm{e}^{-\alpha_x\left|\frac{\omega\xi_x}{U_c}\right| - \alpha_y\left|\frac{\omega\xi_y}{U_c}\right| - \mathrm{j}\frac{\omega\xi_x}{U_c}} \tag{8}$$

where S_p is power spectral density of the wall pressure distribution; U_c is the convection velocity; ξ_x and ξ_y indicate the separation distances of two arbitrary points in the streamwise and spanwise directions on the panel, respectively; α_x and α_y are the decay rates, S_{pp} is the amplitude of the wall pressure fluctuation.

The cabin noises of both the scaled model and the full-scale model were computed for comparison. The thickness of the aircraft panel was 4 mm. The cabin noise is typically determined by the vibration responses of the structure investigated. Thus, two test points on the surface of the model, i.e., P1 and

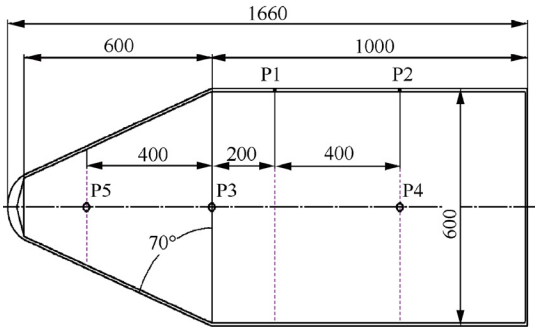

Fig. 2 Distribution of test points corresponding to original model.

P2, were used to measure the structural vibration. The cabin noises were measured at points P3, P4 and P5. The investigated full-scale model was made of aluminum ($E = 7.0 \times 10^{10}$ Pa; $\rho = 2.7 \times 10^3$ kg/m^3; $v = 0.33$), and a scaling coefficient of $\sigma = 0.25$ was chosen. According to the scaling laws derived, the scaled models must also be made of aluminum to satisfy the scaling procedures. The TBL excitation was simulated using the Corcos model, where $\alpha_x = 0.16$, $\alpha_y = 0.46$, $\rho_0 = 1.21$ kg/m^3, $S_{pp} = 1$ Pa, and $U_c = 0.7U_0$, with U_0 being the velocity of the mean flow; here, $U_0 = 30$ m/s. Usually, the Corcos model is only suitable for low-speed flow. However, the TBL excitation used in the scaling procedure is not related to the exact expression of TBL excitation. The Corcos model used here provides only a kind of expression for the TBL excitation, which does not weaken the rationality of the scaling procedure developed. The shell elements were the FEM elements used for computation, and the grid number for the structure was 4753, which ensured that at least 8 nodes existed for a sound wave. Hexahedron grids were applied to compute the internal sound, and the number of acoustic grids used was 1240. The same computation and the comparison of the structural responses were presented in Ref.[19] However, the works in this study focused on the cabin noise prediction.

According to Eq. (4), the cabin noise is mainly determined based on the structure response induced by TBL excitation. However, the results of the structure response were previously given in Ref.[19] and thus will not be re-introduced here. Fig. 3 presents the Sound Pressure Level (SPL) in the cabin of the full-scale model. One result was obtained using the FEM with the full-scale model; the other result was computed using the scaling procedure with the scaled model. Fig. 3 shows that the mean sound levels computed using the two different methods are in good agreement. However, the local sound levels of the two methods, especially for low-frequency noise, have some difference. The reason for this difference is that the computation error usually induces a different cabin noise distribution, and the nonuniformity is more obvious for low-frequency noise because of its lower mode number in bands compared to that of high-frequency noise. However, the mean noise computation can weaken the nonuniform cabin noise distribution. Therefore, the mean noise offers a better comparison compared to the local noise. In Fig. 3, the results based on the scaled model are compared with those obtained with the full-scale model, thus verifying the validity of the scaling procedure derived for the cabin noise prediction.

4. Measurement

The numerical methods typically only provide validation of the scaling equations in theory. For a real structure, many factors might affect the structural vibrations, including the design, manufacturing and installation, resulting in differences from the theoretical response. Thus, two types of experiments were designed to validate the scaling laws derived: a modal test and a wind tunnel test. The modal test was used to measure the modal characteristics of the structure, including the scaled model and the original model. A wind tunnel was used to simulate the TBL excitation of the structure on both the scaled model and the original model.

4.1. Modal test

A modal test was performed to determine the natural vibration of the structure and to provide theoretical support for the revision of the results of the wind tunnel test. For the modal test, a full-scale model with a thickness of 3 mm, which was the same as that of the wind tunnel test model, was made of steel ($E = 2.1 \times 10^{11}$ Pa; $\rho = 7.8 \times 10^3$ kg/m^3; $v = 0.313$). The scaling coefficient for the scaled model, which was made of aluminum ($E = 7.0 \times 10^{10}$ Pa; $\rho = 2.7 \times 10^3$ kg/m^3; $v = 0.33$), was 0.5.

The test points used to measure the structural vibrations and noise distributions in the test model are shown in Fig. 4. The dynamic response of the model was measured under the excitation of an external force generated by a vibration exciter (YMC, Sharker) at F1 and F2 (Fig. 4(a)). The excitation signal was generated by SIGLENT SDG1005 and magnified with a power amplifier (YMC, LA-100). The vibration was detected by accelerometers (PCB, 352C33) mounted at P1 and P2 on the plate shown in Fig. 4, and the internal noise was measured using the microphone (BSWA, MPA 416) located at P3. The signals for the structural vibration and internal noise were collected by a collector (VXI-16026A) and then transferred to a computer.

4.2. Wind tunnel test

The experiment performed in the wind tunnel was designed to utilize the wind tunnel to simulate the TBL excitation more effectively than other methods. The TBL excitation for transonic flows[22–26] is typically more serious. Hence, the

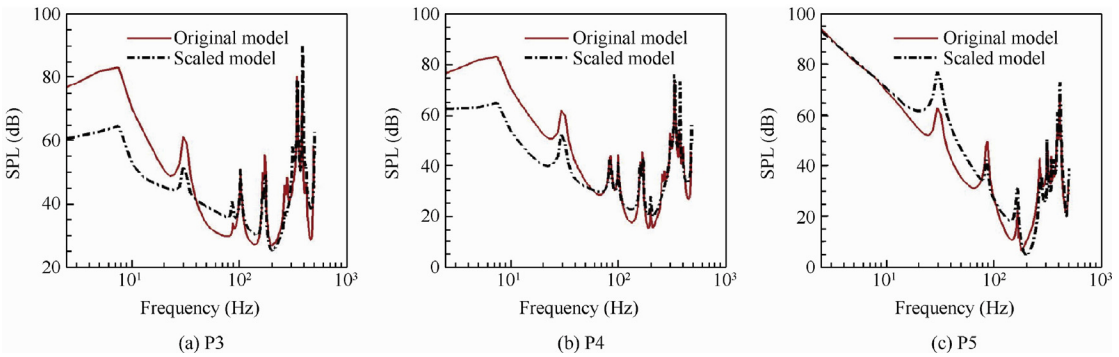

Fig. 3 Sound level prediction with a scaled model under Condition 1.

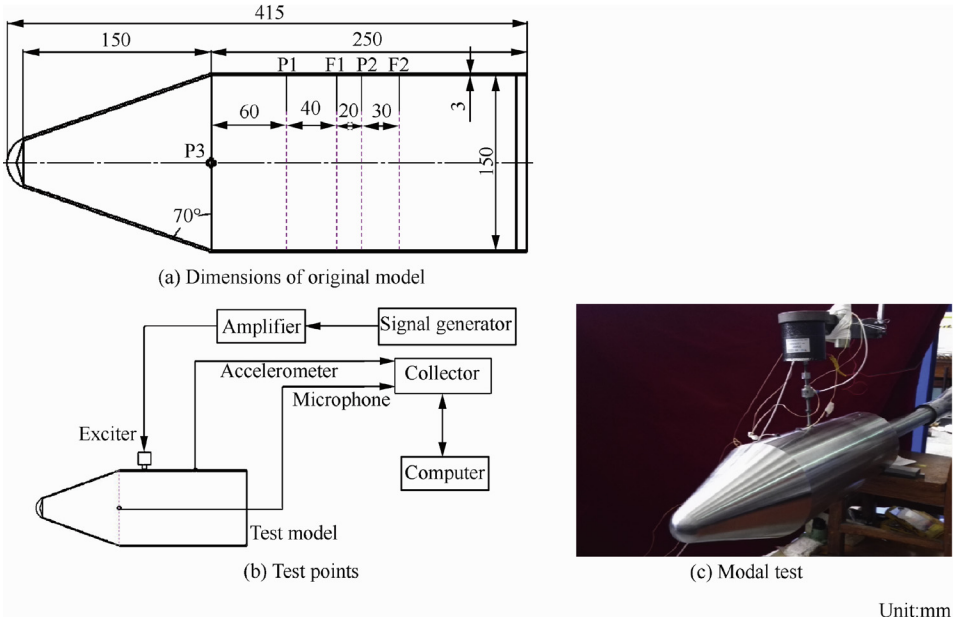

Fig. 4 Experimental test design and model.

TBL excitation of transonic flows was simulated in the wind tunnel to verify the developed scaling procedure. The cabin noise of the full-scale model induced by overflow was compared with the results obtained using the scaling laws with a scaled model to validate the scaling procedures.

The TBL excitation was simulated in the FD-12 wind tunnel, which was built at the China Academy of Aerospace Aerodynamics (CAAA). The FD-12 wind tunnel is a type of intermittent wind tunnel. The dimensions of the wind tunnel are 1.2 m × 1.2 m. The range of the flow Mach numbers simulated in FD-12 is from *Ma* 0.4 to *Ma* 4.0.

For the wind tunnel test, the models used were the same as those used for the modal test in Section 4.1. Because the internal noise of the models was easily influenced by external noise in the wind tunnel, the end of the test model was sealed using the special structure shown in Fig. 5. The model design was presented in Ref.[19] A small hole was maintained in the center of the airproof structure to allow signal transmission. Simultaneously, the support of the test model was designed with sufficient stiffness to avoid model vibrations due to the impact of the airflow in the wind tunnel. For the wind tunnel test, the model was fixed in the middle of the test section to ensure that the model was not affected by the wall of the wind tunnel. Fig. 6 shows the test model fixed in the wind tunnel.

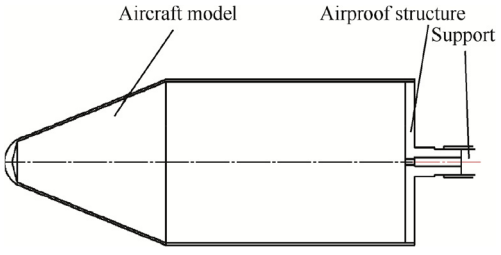

Fig. 5 Design scheme of test model.

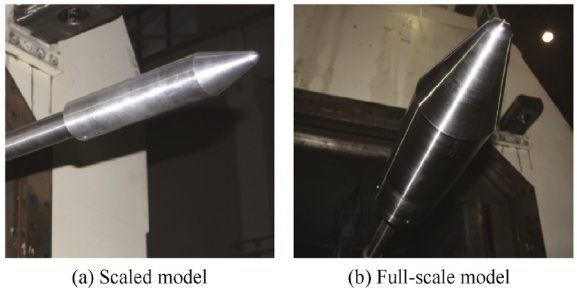

Fig. 6 Test model fixed in wind tunnel.

The test points used for the measurement of structural vibrations and noise distributions in the test model are shown in Fig. 7. The two accelerometers used for the structural vibration measurement were fixed at points PP1 and PP2. Because the structural vibration comparison of the wind tunnel test results had been previously presented in Ref.[19], only the cabin

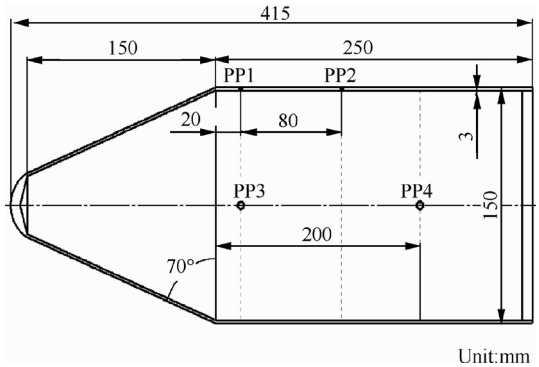

Fig. 7 Distribution of test points corresponding to original model.

noise data were provided to validate the theory. Fluctuating pressure sensors used to measure the internal noise were fixed at points PP3 and PP4. The structural vibration and internal noise were measured with accelerometers (PCB, 333C33) and fluctuating pressure sensors (Kulite XCL-100), respectively. When the wind tunnel was running, the signals for the structural vibration and the cabin noise were collected by a collector (VXI-16026A) and then transferred to a PC.

5. Comparison

Figs. 8 and 9 present the velocity PSD of the model derived from the modal test. The solid line is the test results of the full-scale model, and the dash-dot line was obtained using the scaling laws with the test result of a scaled model. The purpose of the modal test is twofold. The first purpose is to validate the scaling procedure of the cabin noise; the second purpose is to test the frequency offset due to the model manufacture and installation. The frequency offset could be obtained with the test results of the structure response, and the frequency offset should be introduced to compute the cabin noise for a full-scale structure with the scaling procedure. Figs. 10 and 11 show the sound pressure of the cabin under excitation at F1 and F2, respectively. The frequency offsets are considered in Figs. 10 and 11.

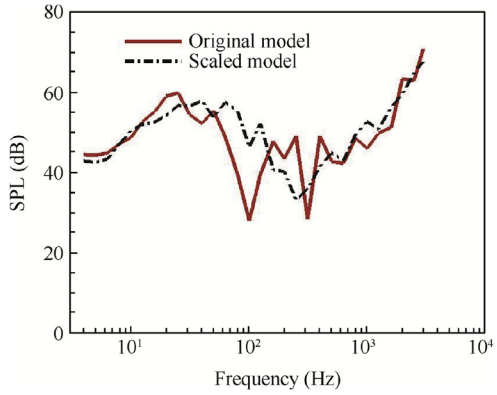

Fig. 10 One-third octave of sound pressure for P3 under excitation at F1.

Figs. 12 and 13 show the 1/3 octave of the cabin noise measured in the wind tunnel of the aircraft model for $Ma = 0.85$ and $Ma = 0.9$, respectively. The results of the scaled model were obtained using the scaling procedure with a scaled model measurement. The results of the original model were obtained via direct measurement of the full-scale model. The results shown, scaled with frequency revision, were obtained using the scaling procedure with the frequency offset considered.

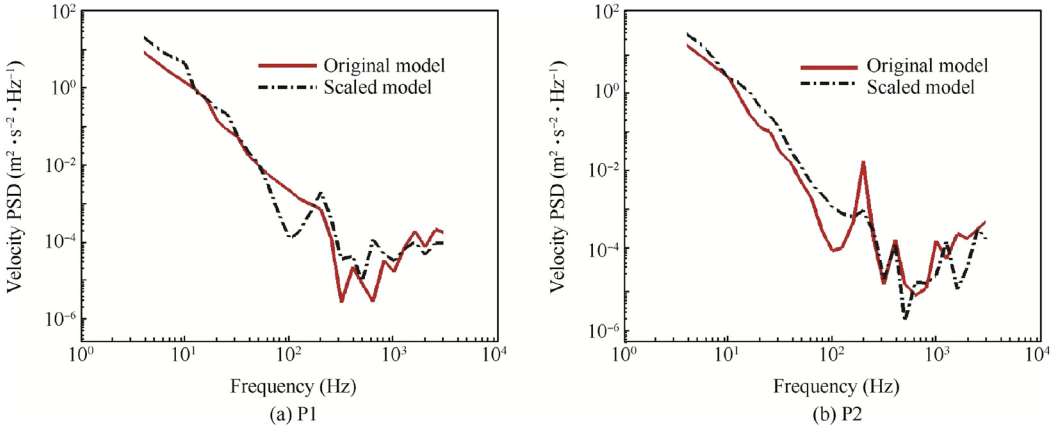

Fig. 8 One-third octave of velocity PSD under excitation at F1.

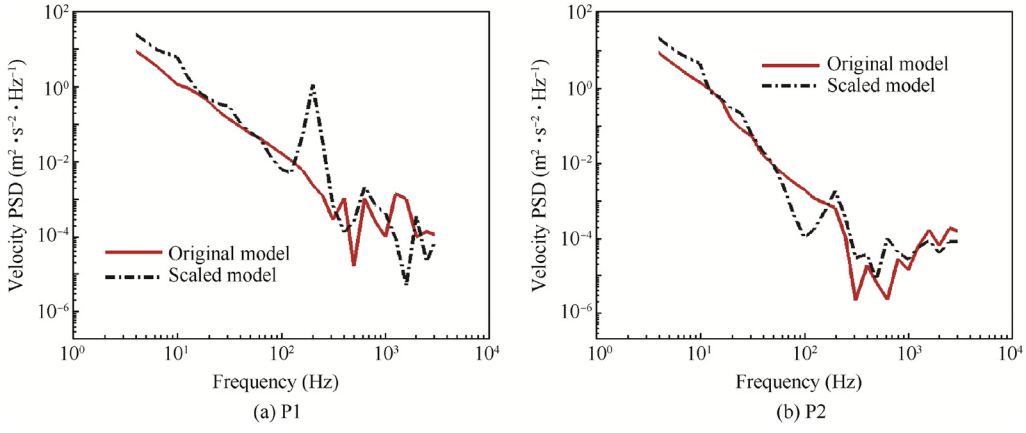

Fig. 9 One-third octave of velocity PSD under excitation at F2.

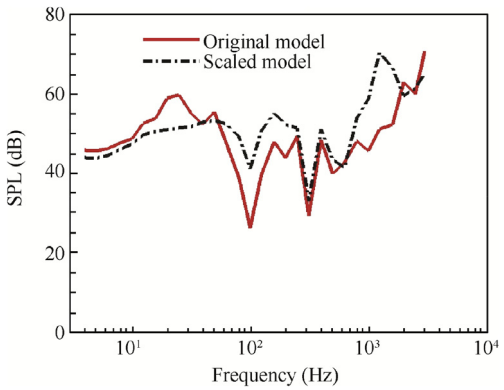

Fig. 11 One-third octave of sound pressure for P3 under excitation at F2.

Figs. 12 and 13 clearly show that a notable frequency offset occurred between the results of the original model and those of the scaled model when the frequency offset was not considered.

The frequency offsets are usually generated for different reasons; the effect of the material used to construct the scaled model on the frequency offset was discussed in Ref.[18] The frequency offset due to the use of different materials can be eliminated via the frequency offset correction shown in Ref.[18] Meanwhile, the errors introduced during the design, manufacture and installation of the structure are also important reasons for generating frequency offsets, particularly in the low-frequency range. However, these errors can be reduced via improvements in the experimental design. This was introduced in Ref.[19] In this paper, the modal test is used for frequency offset correction. In Figs. 12 and 13, the comparisons clearly show that the cabin sound pressure of the aircraft model with the frequency offset considered has a better agreement with the original model results than the scaled model without frequency offset correction.

However, for the cabin sound of the model, the SPL based on the scaled model is in good agreement with the original model results only at point PP3. The background noise may be a factor affecting the sound pressure prediction in the cabin of the models. Although the end of the model was sealed using a special structural design, background noise could still have diffused into the cabin through the hole that was maintained for signal transmission in the support. Because point PP4 is closer to the support than point PP3, it is more easily affected by the background noise of the wind tunnel. The comparison at point PP3 shows more consistent results than that at point PP4.

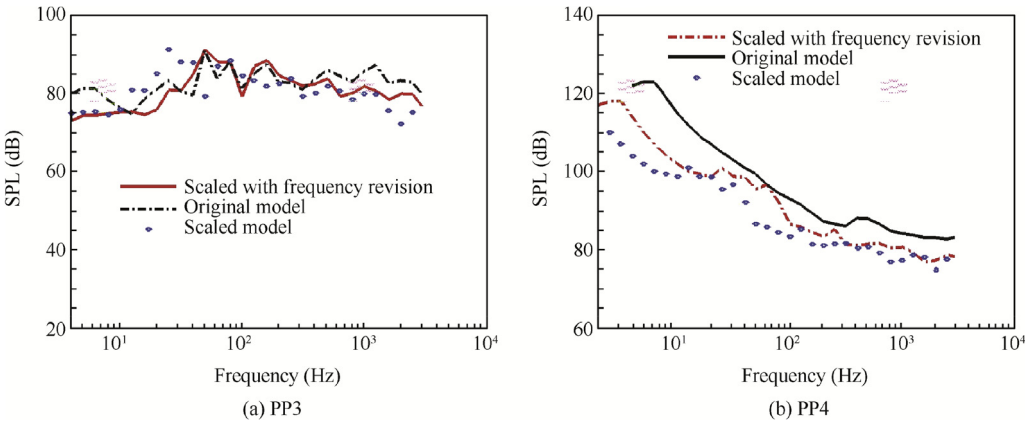

Fig. 12 One-third octave of cabin noise measured in wind tunnel for $Ma = 0.85$.

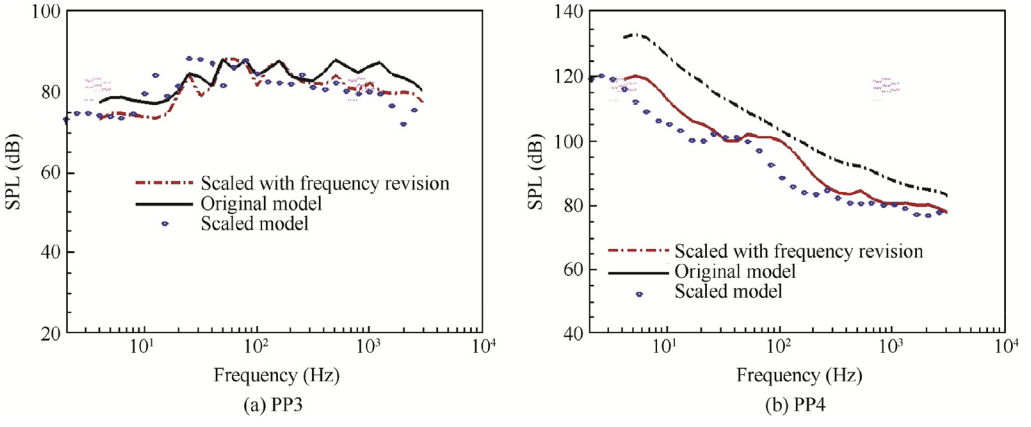

Fig. 13 One-third octave of cabin noise measured in wind tunnel for $Ma = 0.9$.

6. Conclusions

This paper presents a method for scaling cabin sound. The scaling procedure provides an academic foundation for the prediction of the cabin noise of the structure in a wind tunnel. In addition, a new test skill is proposed for investigating cabin noise in a wind tunnel.

The numerical computation provides theoretical results to validate the scaling laws developed for the investigation of the cabin noise generated by TBL excitation on the structure. Because the cabin sound is determined by both the external excitation and the modal characteristic of the structure, a modal test was performed before the wind tunnel test. The modal test provides an effective method to obtain the frequency offset of the structure response due to the model manufacture and installation.

A wind tunnel test was performed to simulate the TBL excitation. The cabin sound of the full-scale model was compared to the results obtained using the scaling procedure based on the scaled model. The comparisons of the measurement results show that the scaling procedures developed in this paper are effective for vibro-acoustic predictions in wind tunnels.

Background noise was an important factor affecting the sound pressure in the cabin of the models for the wind tunnel test. The tail end of test model should be sealed to prevent background noise from entering the cabin of the model. Although the background noise could diffuse into the cabin through the hole that was maintained for signal transmission in the support, a better result might be obtained if a better test scheme was designed.

Symbol	Type	Denotation of superscript and subscript
a, b	scalar	Streamwise and crosswise plate length
h	scalar	Plate thickness
ρ	scalar	Material density
f	scalar	Excitation frequency
D	scalar	Plate stiffness
E	scalar	Young's modulus
v	scalar	Possion's ratio
S_v	function	Velocity power spectral density of plate due to TBL
S_p	function	Power spectral density of the wall pressure distribution
S_{pp}	function	Peak value of TBL excitation
p^i	function	Incidence sound pressure
V	scalar	Free stream velocity
q_∞	scalar	Dynamic pressure of the flow
ζ	scalar	Airy's stress function
a_x, a_y	scalar	Streamwise and crosswise correlation coefficient
ξ_x, ξ_y	scalar	Streamwise and crosswise spatial separation
ω	scalar	Circular excitation frequency
σ	scalar	Scaling coefficient
ρ_0	scalar	Air density
Uc	scalar	Convective velocity
p	scalar	Sound pressure
k	scalar	Wave number
w	function	Normal displacement of the plate

References

1. Corcos GM, Liepmann HW. On the contribution of turbulent boundary layers to the noise inside a fuselage. Washington, D.C.: NACA;1956. Report No.: NACA-TM-1420.
2. Alex LJS. Airplane interior noise modeling using Statistical Energy Analysis Approach. Reston:AIAA;1999. Report No.: AIAA-1999-1903.
3. Joakim H. SAAB'S experience in aircraft interior noise and vibration measurements. Reston:AIAA;1999. Report No.: AIAA-1999-1837.
4. Francesco M, Antonia S, Marco A. Interior noise sources identifications, in-flight measurements and numerical correlations of an advanced business aircraft. Reston:AIAA;2006. Report No.: AIAA-2006-2491.
5. Blakemore M, Heron KH, Davis EB. A new wavenumber-based approach for predicting aircraft cabin noise. Reston:AIAA;2008. Report No.: AIAA-2008-3009.
6. Malte S, Roland E, Olaf H, Oliver U. A synthetic wall pressure model for the efficient simulation of boundary layer induced cabin noise. Reston:AIAA;2010. Report No.: AIAA-2010-3760.
7. Alessandro B, Sebastien G. Semi empirical jet noise modeling for cabin noise prediction-acoustic loads in the geometric near field. Reston:AIAA;2011. Report No.: AIAA-2011-2925.
8. Ferdinand WG. Large Civil Tiltrotor (LCTR2) interior noise predictions due to turbulent boundary layer excita tion. Washington, D.C.:NASA;2013. Report No.: NASA/CR-2013-218005.
9. Nan H, Heino B, Michaela H. Contributions of different aeroacoustic sources to aircraft cabin noise. Reston:AIAA;2013. Report No.: AIAA-2013-2030.
10. Robert GA, Alexey JG. Identification of noise sources in the cabin and determination of the sound energy local passage through the board design based on the results of in-flight measurements of the super jet. Reston:AIAA;2015. Report No.: AIAA-2015-3114.
11. Van Dyke JD, Schendel J, Gunderson C, Ballard M. Cabin noise reduction in the DC-9. Reston:AIAA;1967. Report No.: AIAA-1967-0401.
12. SenGupta G. Methods of reducing low frequency cabin noise and sonically induced stresses, based on the intrinsic structural tuning concept. Reston:AIAA;1977. Report No.: AIAA-1977-0444.
13. Simpson MA. Cabin noise control ground tests for UHB aircraft. Reston:AIAA;1989. Report No.:AIAA-1989-1121.
14. Swanson A, Billoud GD. Aircraft cabin noise reduction through active vibration control. Reston:AIAA;1999. Report No.: AIAA-1999-1935.
15. Maury C, Gardonio P, Elliott SJ. Active control of the flow-induced noise transmitted through a panel. Reston:AIAA;2000. Report No.: AIAA-2000-2042.
16. Julian G, Delf S, Sten B. Global active noise control in aircraft cabins. Reston:AIAA;2009. Report No.: AIAA 2009-3242.
17. Giovanni B, Claudio T, Marco MC. A comprehensive approach for the optimal control of tiltrotor cabin noise through actively-driven piezoelectric actuators. Reston:AIAA;2013. Report No.: AIAA-2013-2032.
18. Zhao XJ, Ai BC, Liu Z, Li D. A scaling procedure for panel vibro-acoustic response induced by turbulent boundary layer. *J Sound Vibrat* 2016;**380**:165–79.
19. Zhao XJ, Ai BC. Predicting the structural response induced by turbulent boundary layer in wind tunnel. *AIAA J* 2017;**55**(4):1221–9.
20. Liu BL, Feng LP, Anders NA. Sound transmission through curved aircraft pannels with stringer and ring frame attachments. *J Sound Vibrat* 2007;**300**:949–73.
21. Liu BL. Noise radiation of aircraft panels subjected to boundary layer pressure fluctuation. *J Sound Vibrat* 2008;**314**:693–711.

Please cite this article in press as: ZHAO X et al. Scaling procedures of cabin noise generated by turbulent boundary layer excitation, *Chin J Aeronaut* (2018), https://doi.org/10.1016/j.cja.2017.12.015

22. Ezra AA, Per-erson HC. Determination of design criteria for transonic buffeting forces acting on launch vehicles. *ARS launch vehicles: structures and materials conference*; Arizona, USA, April 1962.
23. Robertson JE. Unsteady pressure phenomena for basic missle shapes at speeds.Reston:AIAA;1964. Report No.: AIAA-1964-0003.
24. Riddle D. Investigation of surface pressure fluctuation association with buffet. Reston:AIAA;1975. Report No.: AIAA-1975-0067.
25. Serpa JM, Lessmann RC, Hagist WM. Turbulent separated and reattached flow over a curved surface. Reston:AIAA;1986. Report No.: AIAA-1986-1064.
26. Piatak DJ, Sekula MK, Rausch RD. Comparison of ares I-X wind-tunnel derived buffet environment with flight data. Reston: AIAA;2011. Report No.: AIAA -2011-3013.

Please cite this article in press as: ZHAO X et al. Scaling procedures of cabin noise generated by turbulent boundary layer excitation, *Chin J Aeronaut* (2018), https://doi.org/10.1016/j.cja.2017.12.015